Mitigation of Frequency Stability Issues in Low Inertia Power Systems using Synchronous Compensators and Battery Energy Storage Systems

Mitigation of Frequency Stability Issues in Low Inertia Power Systems using Synchronous Compensators and Battery Energy Storage Systems

Carmelo Mosca[1*], Francesco Arrigo[1], Andrea Mazza[1], Ettore Bompard[1], Enrico Carpaneto[1], Gianfranco Chicco[1], Paolo Cuccia[2]

[1] Dipartimento Energia "Galileo Ferraris", Politecnico di Torino, Corso Duca degli Abruzzi, 24, Torino, Italy
[2] North-West Dispatching Area, Terna Rete Italia, Via Sandro Botticelli, 139, Torino, Italy
[*]carmelo.mosca@polito.it

Abstract: The inertia of power systems is a key aspect for frequency dynamics and stability. The increasing penetration of non-synchronous generation reduces the available inertia and makes it fluctuating during the day depending on the online units. This causes problems for grid operators, particularly in relatively small power systems. The present work examines the impact of decreasing inertia using an aggregate model based on the swing equation, considering future lower inertia scenarios and the implementation of the current protection schemes. The frequency stability of the system is assessed by considering the *reference incident*, i.e., the loss of the largest operating unit in under- and over-frequency cases. New solutions to balance the grid are addressed and compared, considering the technical impacts of synchronous compensators (SyC) and Battery Energy Storage Systems (BESSs) operated with a new Equivalent Saturation Logic (ESL). The model is tested and validated using the real data of a small insular power system (Sardinia Island, in Italy), outlining the importance of the HVDC and of the BESS control strategies to guarantee the frequency stability of the power system.

Nomenclature

Acronyms:

BESS	Battery Energy Storage System
COI	Centre of Inertia
ENTSO-E	European Network of Transmission System Operators for Electricity
ESL	Equivalent Saturation Logic
HVDC	High Voltage Direct Current
PFC	Primary Frequency Control
RES	Renewable Energy Sources
ROCOF	Rate Of Change Of Frequency
SACOI	HVDC Sardinia – Corsica – Continent
SAPEI	HVDC Sardinia – Continent
SARCO	AC link Sardinia – Corsica
SyC	Synchronous Compensator
TSO	Transmission System Operator

Parameters and variables:

a	Share of inertia reduction
f	Frequency
f_0	Nominal frequency
f_{nadir}	Nadir frequency
f_{zenith}	Zenith frequency
f_{reg}	Steady-state frequency deviation
x_i	Binary variable containing the *i*-th thermal power plant status
k_{BESS}	BESS virtual inertia response factor
D_L	Change of load under percentage in frequency
E_{BESS}	BESS virtual regulating energy
E_c	Load regulating energy
$E_{k,i}$	*i*-th thermal power plant kinetic energy
$E_{k,sys}$	Kinetic energy of the system
E_p	Permanent regulating energy
H_{BESS}	BESS virtual inertia constant
H_i	Inertia constant of the *i*-th generator
H_{sys}	Aggregated inertia of the system
J	Moment of inertia of the generator
N	Total number of thermal power plants
P_B	BESS nominal active power
P_n	Machine nominal active power
S_L	Total system load
S_{ni}	Rated power of the *i*-th generator
S_{tot}	Total rated power of the generators
T	Pole time constant
T_B	BESS pole time constant
T_{nadir}	Time of nadir frequency
T_{zenith}	Time of zenith frequency
ω_n	Rated rotor mechanical angular velocity
σ_B	Equivalent BESS droop
σ_p	Equivalent power plant droop
τ	Zero time constant
χ_B	BESS inertial control participation share of the total power
Δf	Frequency variation
Δf_{MAX}	Maximum frequency variation
ΔP_{BESS}	BESS power injection
$\Delta P_{B,H}$	Inertial BESS power contribution
$\Delta P_{B,PRI}$	Primary BESS power contribution
ΔP_g	Difference between the generation before and after the incident
ΔP_l	Difference between the load before and after the incident
ΔP_{MAX}	Maximum active power variation

1. Introduction

In the last years, the new policies for the containment of greenhouse gases for 2020 have largely modified the European electric scenario, with an increasing diffusion of plants based on Renewable Energy Sources (RES). The ongoing transition from conventional to non-programmable power sources presents several important challenges for all the actors involved in the energy sector, in particular for electricity [1].

Until now, conventional power plants have been the traditional providers of services that ensure frequency stability (synchronous inertia and governor response). These power plants are being displaced by marginally zero-cost non-synchronous generation, without intrinsic inertial

response [2]. A fundamental difference between traditional and new energy generation is the type of connection to the power system, with non-synchronous connection of a growing number of new generators through power electronic-based devices. Furthermore, the priority dispatch status of non-synchronous renewable generation (wind, wave, photovoltaic, etc.), and the increasing levels of installed High Voltage Direct Current (HVDC) interconnections between synchronous systems, are changing the unit commitment and the economic dispatch order, bringing to the gradual shutdown of large thermal units [2].

The progressive shutdown of the big fossil fuel generation plants is affecting the effectiveness of the frequency regulation that is linked to the instantaneous load-generation balance and to the inertia of the system. One of the main issues with the reduced amount of inertia is frequency stability, defined as the ability of a power system to maintain steady frequency after a severe contingency, causing a considerable imbalance between generation and demand [3]. Such a trend has operational security implications, as systems – particularly isolated systems [4] – may be subject to higher rates of change of frequency (ROCOF) and more extreme frequency oscillations, with reductions in the lowest values (nadir) and increases in the highest value (zenith) of the oscillations following a system disturbance.

The Transmission System Operator (TSO) defines a persistent imbalance caused by a disturbance, outage or network splitting as the "reference incident", i.e., the contingency corresponding to the maximum positive or negative power deviation occurring instantaneously between generation and demand in a synchronous area. The "reference incident" is the basis for the frequency containment reserve calculations and protection scheme settings [5]. A weak frequency stability could first bring to the intervention of current protections, with consistent load and RES shedding, and secondly to stability issues and risk of blackouts. In order to ensure a stable system operation and control, it is necessary to assess the impact of the reduced inertia on the dynamics of power systems. Inertia is closely linked to the dynamics of frequency stability and rotor angle stability [6]. This inertia, related to the rotational masses directly connected (motors and generators) limits the amplitude and speed of frequency perturbation following unbalance between load and generation, particularly in the first moments after the perturbation. Subsequently, new ancillary services and technical solutions are required to reduce the unbalance and restore the nominal value of grid frequency, as reported by ENTSO-E [5]. In this context, synchronous compensators (SyC) [7], [8], and Battery Energy Storage Systems (BESS) represent interesting solutions to maintain the stability of the power system adding real or virtual inertia [9].

The effect of SyC for frequency stability enhancement has been investigated in [10] for a system with high level of renewable energy penetration, using different scenarios of wind and disturbances, showing satisfactory performance. Recently, also some approaches for improving the frequency support from BESS have been investigated [11]. Some studies pointed out that BESS are a promising technology for ancillary services provision, particularly on Primary Frequency Control (PFC) [12]. Due to their speed and precision in regulating their active power, BESS can be used also to provide inertial response, giving virtual inertia to the grid and using different control strategies [13], [14]. However, little attention has been paid to the selection of the contingency and the definition of future scenarios and parameters for the BESS control. Although detailed dynamic models have been used [10], [15], aggregate models [16], [17], have shown their accuracy and fast performance, when the primary interest is mainly in the maximum frequency deviation and the time taken to reach it [18]. Nevertheless, they could lack of validation on real events and implementation of real frequency protection schemes. Table 1 summarises the characteristics of the above indicated references, comparing them with the present work.

This paper highlights the impact of variable inertia on the dynamics of frequency stability using an aggregate model to analyse over and under frequency response, considering the effects of SyC and BESS on the frequency evolution. An enhanced modelling of the BESS behaviour is given, where the available power band is divided between primary and inertial intervention and the parameters are set using a new Equivalent Saturation Logic. The model incorporates also HVDC and real protection schemes. The model is tested and validated using the real data of the insular power system of the Sardinia Island, in Italy, comparing past and future generation scenarios in a transmission system with high share of RES.

Table 1 Comparisons among references that consider Syc/BESS

Ref.	System	Scenarios, contingencies and protection schemes	Dynamic Models	Options	BESS Control Strategy
This paper	Real (Sardinia)	Future scenarios obtained using optimization. Reference incident. Actual protection schemes.	Aggregate model with calibration on a real event.	SyC & BESS	Inertial and primary support. Fixed droop strategy. Equivalent Saturation Logic.
[8]	In-house GB system	Only one scenario. No protection schemes.	Not specified.	SyC	-
[10]	Real (Western Denmark)	Generic scenarios. No protection schemes.	Real Time Simulator.	SyC	-
[13]	Generic	Three generic case studies. No protection schemes.	DigSilent model.	BESS	Sensitivity analysis on inertial response.
[15]	IEEE 39 system adapted to the Irish power system	No future scenarios. Loss of the largest synchronous generator. No protection schemes.	DigSilent model and calibration on real event.	BESS	Sensitivity analysis on the control parameters.
[16]	Generic	Two general scenarios with high and low inertia. No protection schemes.	Aggregate model.	BESS	Primary support. Sensitivity analysis on the control parameters.
[17]	Real (Mexico)	No future scenarios, only test cases. Generator and load disconnection. No protection schemes.	Aggregate model.	BESS	Inertial and primary support.

The contributions of the paper are summarized in the following points:

- Implementation of an aggregate model based on the insular power system of the Sardinia Island. HVDC, BESS, SyC and the real frequency protection schemes for frequency stability are considered in the model and a validation on a real event is performed.
- The reference incident is considered in future inertia scenarios, built using an optimization approach, for both under and over frequency phenomena, and it varies according to the particular situation of the system.
- A new Equivalent Saturation Logic is used to tune the control parameters of the BESS in an effective way and the available power band is divided between primary and inertial intervention, performing a sensitivity analysis.

The outline of this paper is as follows. Section 2 gives a brief overview of the primary frequency control schemes and models used. Section 3 describes the indexes used to evaluate the impact of the reference incident. Section 4 outlines how the scenarios are developed. The case study and the simulation results are presented in Section 5. Section 6 reports the concluding remarks and future research ideas.

2. Aggregate dynamic model

The traditional frequency regulation schemes in continental Europe are generally organised into a hierarchical structure including primary, secondary and tertiary regulations, which act on different, increasingly slower time scales [19]. When a power unbalance occurs, in the first instances, the missing power is immediately balanced by the rotational inertia, and then the primary regulation contrasts the frequency variation [20]. After a disturbance in the system, like a loss of generation, the frequency in different parts of a large power system varies with different oscillations. The frequency variations of the different machines can be regarded as small variations over an average frequency in the system. This average frequency, called the system frequency, is the frequency that can be defined for the so-called Centre of Inertia (COI) of the system [21]. The basic concept of the aggregate model is based on the idea of this uniform or average frequency, where oscillations between generators are filtered out, but the average frequency behaviour is retained [22]. This holds under the assumption that generators maintain their rotor angle stability with respect to each other (grid synchronism), which has been well observed in actual power systems [23]. Such a model is based on the swing equation for the set of synchronous machines in the system.

$$\frac{df}{dt} = \frac{f_0}{2H_{sys}S_{tot}}(\Delta P_g - \Delta P_l) \tag{1}$$

where f_0 is the system frequency prior to the incident [Hz], H_{sys} is the aggregated inertia of the system [s], S_{tot} is the total rated power of the generators [MW], ΔP_g is the difference between the generation before and after the incident and ΔP_l is the difference between the load before and after the incident [MW]. In particular:

$$H_{sys} = \frac{\sum_{i=1}^{N} S_{ni}H_i}{S_{tot}} \tag{2}$$

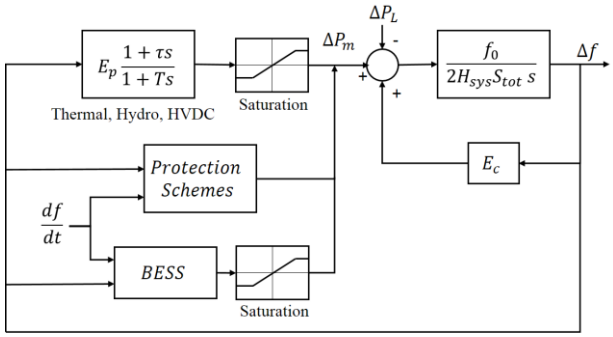

Fig. 1. *Main components of the aggregate model.*

$$S_{tot} = \sum_{i=1}^{N} S_{ni} \tag{3}$$

where S_{ni} is the rated power of generator i [MW] and H_i is the inertia constant of generator i [s]. For a synchronous generator, H_i is defined as the ratio between the stored energy at rated speed E_{ki} and the rated apparent power of generator i [3]:

$$H_i = \frac{1}{2}\frac{J\,\omega_n^2}{S_{ni}} = \frac{E_{ki}}{S_{ni}} \tag{4}$$

where J is the moment of inertia of the generator [kg×m^2] and ω_n is the rated mechanical angular velocity of the rotor [rad/s]. Instead of expressing inertia of a power system in seconds, it is often more convenient to calculate the kinetic energy stored in rotating masses of the system, expressed as:

$$E_{k,sys} = S_{tot}H_{sys} = \sum_{i=1}^{N} S_{ni}H_i \tag{5}$$

Using these considerations, a linearized power system model is developed, where an equivalent power plant is adopted to represent all the synchronous generators present in the system, divided in thermal and hydro units [22]. The model is formed by:

1. System inertia.
2. Equivalent traditional power plant transfer function with a pole and a zero.
3. Primary frequency control model.
4. Frequency-dependent loads.

The block parameters are:

- The equivalent power plant zero time constant τ [s].
- The equivalent power plant pole time constant T [s].
- The constant describing the system inertia $\frac{f_0}{2H_{sys}S_{tot}}$ $[\frac{MWs}{Hz}]$.
- The permanent regulating energy $E_p = -\frac{P_n}{f_0\sigma_p}$ [MW/Hz], where σ_p is the equivalent power plant droop and P_n is the machine nominal active power.
- The constant load regulating energy $E_c = D_L S_L$ $[\frac{MW}{Hz}]$, where D_L is the change of load under percentage in frequency and S_L is the total load of the system.

In general, the frequency dependency of the aggregated system load is clearly observable, with a stabilizing effect on

Table 2 Dynamic Data

Equipment	Zero time constant τ [s]	Pole time constant T [s]	Droop [%]	Band [MW]
Thermal	3	10	5%	0.1 P_n
Hydro	-1	6	4%	0.1 P_n
HVDC	3.3	10	5%	P_{max}

the frequency. Loads have a component depending directly on frequency and an additional contribution depending on the derivative of frequency (e.g., kinetic energy stored in industrial motor loads) [21]. In this paper, only the first effect is modelled with E_c, as the Sardinian power system does not supply large rotating motor loads, due to the current absence of widespread large industrial customers. Furthermore, in the future the contribution of loads to inertia will be much lower, due to the massive penetration of electronic converters to control rotating motor loads.

The proposed aggregate dynamic model has been modified and extended with respect to the ones found in the literature, e.g. [22], by including the response of the HVDC, BESS and SyC. The real protection schemes and thresholds are based on the ones adopted by ENTSO-E [19], [24], [25], with different shedding shares of load and generation depending on frequency values:

- Wind shedding, starting from 50.6 Hz.
- Hydro shedding, activated at 51 Hz.
- Pump shedding, starting from 49.5 Hz.
- Interruptible load shedding, at 49.3 Hz.
- Automatic load shedding, for extreme situations from 48.8 Hz.

2.1. Dynamic characteristic of the grid

Table 2 contains the parameters to set the dynamic model of thermal, hydro and HVDC units, considering a zero-pole dynamic, a fixed droop and the power band coming from the Italian grid code requirements (10% of the maximum power). The HVDC reserve depends on the operating conditions, and it varies if the link is importing or exporting, according to the maximum and minimum operation point. Different time constants were chosen to model the different primary power response behaviour of thermal, hydro and HVDC units.

In the aggregate model, synchronous compensators contribute to increase the kinetic energy in the system through the parameters H_{sys} and S_{tot}, without providing primary control, while BESS are able both of providing synthetic inertia and primary frequency control. In this work, each SyC is characterised by an inertia constant of 2 s and an apparent power of 250 MVA. The main components of the aggregate model can be seen in Fig. 1.

2.2. Dynamic model of a BESS

The dynamic model for the BESS is shown in Fig. 2. The BESS model derives from [16], with the difference that the contribution due to the derivative of frequency is instantaneous, to emulate the inertial synchronous response.

The component related to Δf is the primary frequency control level, whereas the component related to df/dt aims to simulate the virtual inertia. The battery primary control is modelled as a first order transfer function [11], which is suited for power system stability studies.

The block parameters are:

- The virtual regulating energy of the BESS, $E_{BESS}=-\frac{P_B}{f_0\sigma_B}$ where σ_B is the equivalent BESS droop and P_B is the BESS nominal active power.
- The equivalent BESS pole time constant T_B.
- The BESS virtual inertia response factor, defined as $k_{BESS} = \frac{2\,H_{BESS}P_B}{f_0}$.

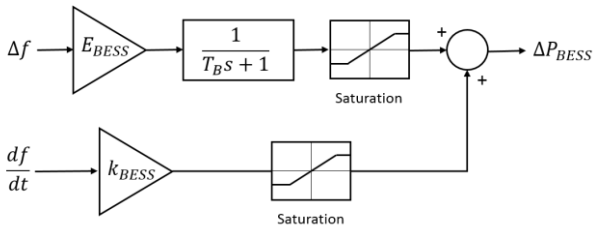

Fig. 2. *Dynamic model of a BESS*

- The BESS power injection for regulation ΔP_{BESS}, that can be divided in the inertial contribution $\Delta P_{B,H}$ and primary contribution $\Delta P_{B,PRI}$.

A Fixed Droop strategy is considered as control strategy of the BESS. Therefore, in PFC a lower droop can be used, much more performing with respect to the usual value of the traditional generation [26]. In the case of conventional plants, as mentioned earlier, the band reserved for PFC is $\frac{\Delta P_{MAX}}{P_n} = 10\%$ in Sardinia, whereas BESS use 100% of their band. Consequently, a new equivalent value for the droop can be computed, imposing for the BESS the saturation of its reserve at the same frequency deviation of a conventional unit but with $\left(\frac{\Delta P_{MAX}}{P_n}\right)_B = 1$. The frequency at which the reserve is saturated is computed as:

$$\Delta f_{MAX} = \frac{\Delta P_{MAX}}{P_n} f_0 \sigma_p \tag{6}$$

$$\sigma_B = \frac{\Delta f_{MAX}}{f_0}\left(\frac{P_n}{\Delta P_{MAX}}\right)_{BESS} = 0.005 \tag{7}$$

With this new value, it is possible to compute the equivalent regulating energy of the BESS, considering as P_B the share of participation in PFC of the total power.

This BESS model is appropriate to capture the major dynamic during the contingency and evaluate the impact of the BESS on the grid. A specific contribution of this work is the use of an Equivalent Saturation Logic to calculate the virtual inertia contribute H_{BESS} of the BESS, which is used for the calculation of k_{BESS} using the hypothesis of the saturation for an extreme ROCOF of 1 Hz/s [27]. The idea is to replicate the inertial behaviour of the synchronous generators, which produces an instantaneous active power variation for every value of ROCOF in the system. In the case of the BESS, a conventional extreme ROCOF is decided and the active power variation is imposed as the maximum available. Therefore, it is possible to calculate the virtual inertia contribution H_{BESS}

$$H_{BESS} = \frac{f_0\,\chi_B}{2\left|{}^{df}/_{dt}\right|_{MAX}} \tag{8}$$

where χ_B is the share of participation in the inertial control of the total power of the BESS, whereas 1-χ_B represents the share of participation in the primary control.

Four different strategies for BESS simulation are used, based on active power band devoted to inertial or primary control:

1. 50% of active power used for inertial and primary control $\chi_B = 0.5$, with two different pole time constant.
   i. T_B = 0.1 s.
   ii. T_B = 0.3 s.
2. Only inertial control $\chi_B = 1$.
3. Only primary control $\chi_B = 0$ with T_B = 0.3 s.

3. Impact of the reference incident

The frequency stability of the system is assessed by considering the reference incident. The reference incident is the loss of the largest operating unit, both in the case of under-frequency and over-frequency and it depends on the size of the grid. In a small power system, as the Sardinian one, the N-1 security is evaluated each 15 minutes considering the upward and downward reserve, according to the current dispatch. The largest lost operating unit can be either the largest thermal power plant or the HVDC connection, depending on the operating conditions.

The real measurements provide the initial condition of each generator and are used for the frequency dynamic studies as input for the aggregated model. The initial condition for the frequency stability assessment of the system is considered from the standard 50 Hz. The impacts are evaluated considering the value of maximum frequency excursion (in terms of nadir/zenith) and ROCOF, compared to the limits. The limits considered are:

1. 50.6 Hz in over-frequency (wind shedding threshold)
2. 49.3 Hz in under-frequency (interruptible load shedding)
3. 0.5 Hz/s for ROCOF, as prescribed by the ENTSO-E standard [29].

The aggregate dynamic model has been developed, using MATLAB and Simulink, to study primary system-frequency dynamics during the initial post-contingency timeframe. Our analysis is limited to the first 30 seconds after the unbalance, where the highest stress for frequency stability is usually detected [28]. Therefore, only the primary frequency control is considered, as the primary response shall be fully activated in less than 30 seconds [19].

The performance of the frequency response is assessed in terms of the following indicators:

- Maximum transient frequency deviation, denoted as f_{nadir} for under-frequency or f_{zenith} for over-frequency phenomena.
- Time of nadir or zenith frequency (T_{nadir}, T_{zenith}).
- Initial ROCOF, evaluated using (1).
- Steady-state frequency deviation f_{reg}.
- Time of steady-state frequency deviation, evaluated as the time where the frequency is within a band of f_{reg}±0.005 Hz, i.e., one half of the dead band of the generators [19].

4. Future Scenarios

To simulate different low inertia situations, an appropriate strategy has been implemented to identify which units can be switched off in order to obtain a given reduction of kinetic energy. The system kinetic energy is reduced by opening some thermal power plants and replacing their production with the variation on the HVDC links or the increase of wind generation. Three possible future scenarios are taken into account in this paper. Starting from the present situation, the power system inertia is reduced of 10, 30 and 50%.

In order to maintain the situation as real as possible, obtaining the desired percentage of reduced kinetic energy, the following mixed-integer linear programming (MILP) minimization problem is outlined:

$$\min\left\{a \cdot E_{k,sys} - \sum_{i=1}^{N} E_{k,i} \cdot x_i\right\} \quad (9)$$

$$\text{s.t. } x_i \in (0,1) \text{ for } i = 1, \ldots, N$$

where a [pu] is the share of inertia reduction (e.g., 0.1, 0.3 and 0.5), N is the total number of thermal power plants in the system, x_i is a binary variable containing the i-th thermal power plant status for $i = 1, 2, \ldots N$, whose components are 0 if the plant is open or 1 if the plant is closed, $E_{k,sys}$ [MWs] is the amount of present situation kinetic energy and $E_{k,i}$ [MWs] contains the kinetic energy for the i-th thermal power plant. The scope is to minimize the difference between the desired kinetic energy reduction (expressed as the percentage a of the total kinetic energy) and the kinetic energy given by the actual power plants present in the system. For the new values of kinetic energy, the effects of the reference incident are evaluated and compared to the present situation.

5. Case study

The Sardinian power system is considered as a realistic and interesting case study thanks to the fact that it is a small power system (maximum load around 1500 MW). The Sardinia Island is connected to the continental grid through two HVDC systems, named SACOI (Sardinia-Corsica-Italy) and SAPEI (Sardinia-Peninsula). Both HVDC links can modify active power exchanges depending on the frequency variations of the Sardinia grid. The Corsica power system is synchronized to Sardinia through the Sardinia-Corsica (SARCO) AC link.

Considering the high share of RES, the HVDC links and the storage systems, the Sardinian power system contains the main innovative features of the future power systems. Reference [30] gives an overview of the Sardinian generation, demand and transmission system in the context of the high penetration of RES. Furthermore, a dedicated control solution

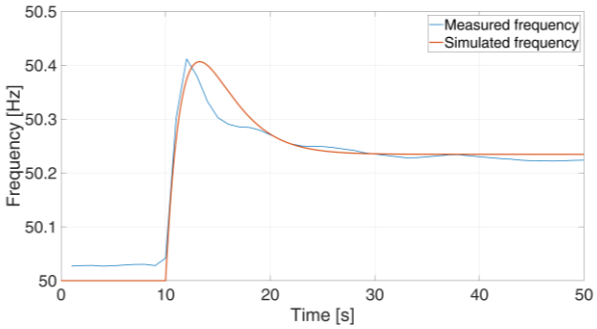

a. Over-frequency event

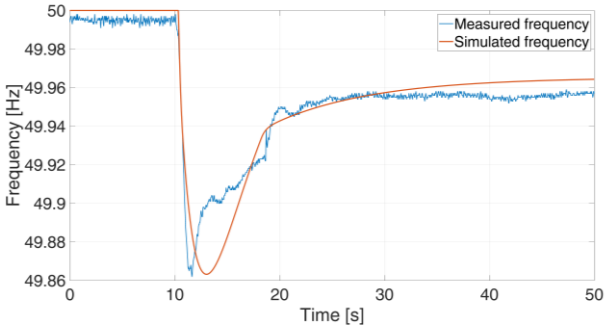

b. Under-frequency event

Fig. 3. *Frequency comparison.*

Table 3 Calibration Results Comparison

a. Over-frequency event	Measured	Simulated
Zenith [Hz]	50.41	50.41
ROCOF [Hz/s]	0.36	0.37
T_{zenith} [s]	2	3.26
f_{reg} [Hz]	50.22	50.23

b. Under-frequency event	Measured	Simulated
Nadir [Hz]	49.86	49.86
ROCOF [Hz/s]	0.76	0.80
T_{nadir} [s]	1.63	3.03
f_{reg} [Hz]	49.96	49.96

for a three-terminal VSC HVDC which enhances the Sardinian frequency stability is studied in [31].

5.1. Comparison with an actual system disturbance

The aggregate model was calibrated using real events. In Fig. 3, the comparison between the simulated and actual frequency response for two failures is reported: a SACOI HVDC failure in 2018 (a) and a thermal unit failure in 2019 (b). The SACOI power flow was in export, so an over-frequency event occurred. The under-frequency is related to the thermal unit failure.

Table 3 summarises the results of the comparison reported in Fig. 3 for the over-frequency and under-frequency events. In both cases, the values for zenith/nadir, ROCOF, and steady-state frequency obtained from the simulations match very well the measured ones. The timings for zenith or nadir are less precise; however, this does not imply major concerns, as currently the TSOs consider more relevant the ROCOF and maximum frequency deviation to assess the frequency stability.

5.2. Simulations and results

The frequency stability of the system is assessed by considering under and over-frequency events in past and future scenarios in terms of low inertia and the technical impact of SyC and BESS. A sensitivity analysis is performed on the quantity of primary and inertial response provided by BESS. The different scenarios have been simulated in a reference day of the year, i.e. the winter peak on 17 January 2018 at hour 10:30 for:

1. Over-frequency event due to the HVDC SAPEI failure.
2. Under-frequency event due to the largest thermal unit failure.

In general the periods of low load and high wind availability are the most problematic scenarios [32], [33].

Table 4 Situations with BESS addition

10 – 30 – 50% Reduced Inertia			
n	MW	T_B	χ_B
1	0	0	-
2	50	0.3	0.5
3	50	0.1	0.5
4	50	0.3	1
5	50	0.3	0
6	100	0.3	0.5
7	100	0.1	0.5
8	100	0.3	1
9	100	0.3	0

However, the Sardinia island is managed covering the load with traditional synchronous generators, while all the wind produced power is exported to the continent through the two HVDCs, which represent the highest contribution in the regulating energy of the island. For the particular condition of the Sardinian system in the chosen day, the situation could have been very critical because the HVDC SACOI was out of service. The worst-case contingency for over-frequency is the HVDC SAPEI failure, which was in export. The HVDC SAPEI was operated in bipolar mode, so the worst contingency is the one pole failure, and the other one can still regulate.

First, the frequency behaviour in the two cases is analysed with some considerations on the phenomena involved and the evaluation of the parameters of interest. The future scenarios of kinetic energy are applied, replacing the thermal generation with the same increase of wind production and the same contingency is simulated. The performance of frequency regulation are assessed using the indicators given in Section 3. With reduced inertia scenarios, the situation is worse for nadir and ROCOF, whereas the steady-state time decreases, because the system has less regulating energy to maintain its condition after an event. To improve the situation, synchronous compensators and BESSs are added. The case of 6 and 10 synchronous compensators (in the initial situation only 2 compensators are present) and two systems of 50 MW and 100 MW BESSs are analysed. For the BESS a sensitivity analysis is carried out with different values of regulating energy and the dynamic pole constant. The frequency response of the BESS is compared using different shares of inertial and primary response, i.e., 50% of inertial and primary control, 100% inertial control and 100% of primary control. The situations considering BESS addition are summarised in Table 4.

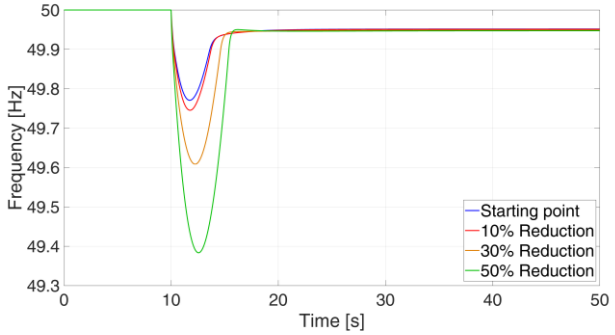

Fig. 4. *Comparison of the impact of the worst-case under-frequency contingency for the scenarios and the actual situation.*

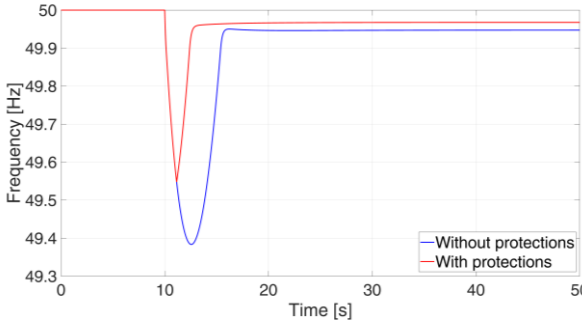

Fig. 5. *Comparison of the impact of the worst-case under-frequency contingency for 50% reduced inertia scenario with and without the implementation of actual protection schemes.*

Table 5 Results of the under-frequency scenario with 10% reduced inertia

Starting situation					
n	Nadir [Hz]	ROCOF [Hz/s]	T_{nadir} [s]	T_{reg} [s]	f_{reg} [Hz]
1	49.75	0.606	1.78	7.99	49.951
Addition of Synchronous Compensators					
n	Nadir [Hz]	ROCOF [Hz/s]	T_{nadir} [s]	T_{reg} [s]	f_{reg} [Hz]
6	49.77	0.505	1.89	7.8	49.951
10	49.78	0.433	2.01	7.6	49.951
Addition of BESS					
n	Nadir [Hz]	ROCOF [Hz/s]	T_{nadir} [s]	T_{reg} [s]	f_{reg} [Hz]
2	49.80	0.566	1.48	8.96	49.952
3	49.80	0.566	1.50	8.96	49.952
4	49.76	0.530	1.86	7.85	49.951
5	49.82	0.606	1.19	9.33	49.953
6	49.83	0.530	1.28	9.33	49.953
7	49.84	0.530	1.30	9.29	49.953
8	49.77	0.471	1.94	7.71	49.951
9	49.86	0.606	0.86	9.59	49.955

Table 6 Results of the under-frequency scenario with 30% reduced inertia

Starting situation					
n	Nadir [Hz]	ROCOF [Hz/s]	T_{nadir} [s]	T_{reg} [s]	f_{reg} [Hz]
1	49.61	0.776	2.25	5.56	49.949
Addition of Synchronous Compensators					
n	Nadir [Hz]	ROCOF [Hz/s]	T_{nadir} [s]	T_{reg} [s]	f_{reg} [Hz]
6	49.67	0.618	2.31	5.56	49.949
10	49.71	0.513	2.37	5.87	49.949
Addition of BESS					
n	Nadir [Hz]	ROCOF [Hz/s]	T_{nadir} [s]	T_{reg} [s]	f_{reg} [Hz]
2	49.73	0.711	1.58	5.56	49.949
3	49.75	0.711	1.58	9.05	49.950
4	49.65	0.656	2.29	5.67	49.949
5	49.77	0.776	1.18	9.55	49.951
6	49.79	0.656	1.29	9.51	49.951
7	49.80	0.656	1.33	9.48	49.951
8	49.69	0.568	2.34	5.77	49.949
9	49.83	0.776	0.82	9.81	49.953

5.2.1 Under-frequency event: In the starting condition, the frequency nadir occurs at 49.77 Hz and the ROCOF is 0.56 Hz/s. Fig. 4 shows the frequency behaviour in the initial situation and the considered scenarios. As expected, the frequency performance is worse in the 50% reduced inertia scenario. In particular, Fig. 5 shows that the 50% reduced inertia scenario is the only one in which the protection schemes are activated, with the pump shedding at 49.5 Hz.

Some tests have been carried out, to show the different improvements that could be reached adding SyC and BESS. The results for the different scenarios are reported in Tables 5, 6 and 7.

In the 10% reduced inertia case (Table 5), it would not be necessary to add components to the power system, meaning that a reduction of 10% of the actual kinetic energy of the Sardinia is possible. Similar considerations are applicable to the 30% reduced inertia scenario (Table 6).

In the 50% reduced inertia scenario (Table 7), the frequency nadir changes from 49.77 Hz to 49.38 Hz. The ROCOF value passes from 0.56 Hz/s to 1.07 Hz/s, making the situation dramatically worse. The addition of SyC increases the inertia of the power system affecting both frequency nadir and ROCOF. It is evident that the steady state frequency does not change, connected to the missing regulating energy capacity of the synchronous compensators.

With 10 synchronous compensators, the frequency nadir improves 0.4% with respect to the initial value.

Better values of nadir frequency and ROCOF are obtained if the BESS capacity is higher. The frequency response of 50 MW of BESS is compared using different pole time constants, i.e., $T_B = 0.1$ s and $T_B = 0.3$ s, with 50% of inertial and primary control. Only a little difference is observed, showing that the time pole constant does not have relevant effect on the situation.

Using only inertial control (n = 4) leads to the best situation for ROCOF (which changes from 1.066 Hz/s to 0.850 Hz/s) but the lowest improvement of the nadir frequency (which changes from 49.38 Hz to 49.49 Hz). On the contrary, using only primary control (n = 5) gives the best situation for the frequency excursion (from 49.38 Hz to 49.71 Hz) but the ROCOF does not basically change from the initial situation (around 1.07 Hz/s). A compromise is reached with the same share of inertial and primary control (n = 2), having a new value for frequency nadir of 49.63 Hz and for ROCOF of 0.95 Hz/s.

In Fig. 6, the values of frequency nadir and ROCOF are reported with respect to the different shares of reduced inertia, starting from the situation without adding BESS (n = 1) and the other situations listed in Table 3. The worst-case under-frequency contingency is compared to the actual situation, represented by the dashed line. In all situations, the addition

Table 7 Results of the under-frequency scenario with 50% reduced inertia

Starting situation					
n	Nadir [Hz]	ROCOF [Hz/s]	T_{nadir} [s]	T_{reg} [s]	f_{reg} [Hz]
1	49.38	1.066	2.57	5.78	49.947
Addition of Synchronous Compensators					
n	Nadir [Hz]	ROCOF [Hz/s]	T_{nadir} [s]	T_{reg} [s]	f_{reg} [Hz]
6	49.52	0.787	2.57	5.78	49.947
10	49.60	0.623	2.72	6.11	49.947
Addition of BESS					
n	Nadir [Hz]	ROCOF [Hz/s]	T_{nadir} [s]	T_{reg} [s]	f_{reg} [Hz]
2	49.63	0.946	1.85	9.07	49.949
3	49.64	0.946	1.85	9.02	49.949
4	49.49	0.850	2.63	5.90	49.947
5	49.71	1.066	1.11	9.80	49.950
6	49.74	0.850	1.23	9.73	49.950
7	49.76	0.850	1.26	9.66	49.950
8	49.56	0.707	2.68	6.02	49.947
9	49.79	1.066	0.72	9.97	49.952

Table 8 Results of the over-frequency scenario with 50% reduced inertia

Starting situation					
n	Zenith [Hz]	ROCOF [Hz/s]	T_{zenith} [s]	T_{reg} [s]	f_{reg} [Hz]
1	51.10	1.091	3.85	12.46	50.052
Addition of Synchronous Compensators					
n	Zenith [Hz]	ROCOF [Hz/s]	T_{zenith} [s]	T_{reg} [s]	f_{reg} [Hz]
6	50.86	0.806	4.01	12.93	50.052
10	50.71	0.638	4.12	9.34	50.052
Addition of BESS					
n	Zenith [Hz]	ROCOF [Hz/s]	T_{zenith} [s]	T_{reg} [s]	f_{reg} [Hz]
2	50.68	0.969	2.99	6.89	50.051
3	50.67	0.969	3.00	6.94	50.051
4	50.91	0.871	3.97	9.09	50.052
5	50.49	1.091	2.10	9.80	50.050
6	50.42	0.871	2.15	9.63	50.050
7	50.39	0.871	2.16	9.46	50.050
8	50.79	0.724	4.06	9.25	50.052
9	50.28	1.091	0.81	10.43	50.048

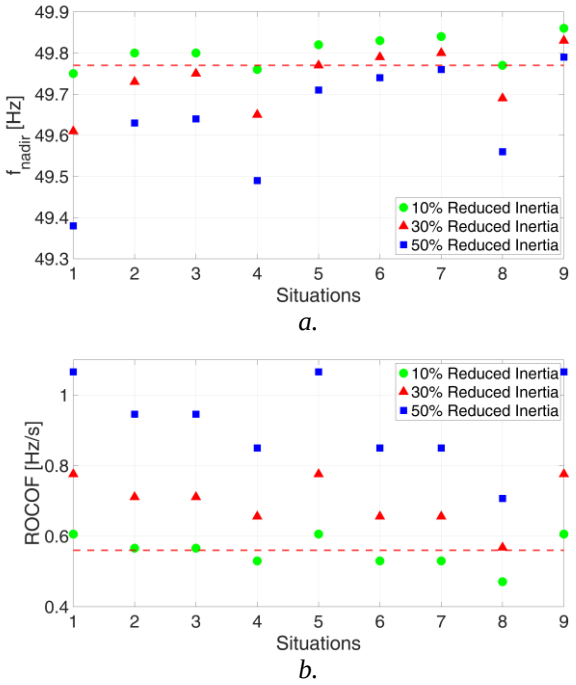

Fig. 6. *Comparisons of the impacts of the worst-case under-frequency contingency for the scenarios and the actual situation, considering the 9 different situations listed in Table 3. The dashed line is the current situation.*

of BESS improves the performance of the system. In terms of increasing the frequency nadir, the situation 9, with the addition of 100 MW of BESS used only for primary frequency control, shows the best performance. Conversely, the situation 8, with the same BESS used only for inertial control provides only slight improvements with respect to the initial situation 1. From Fig. 6a, similar considerations hold for the comparison between situation 5 and 4 with 50 MW of BESS. In the intermediate situations with 50% of inertial and primary frequency control, the results tend to be similar to the situation with only primary frequency control.

With reference to ROCOF (Fig. 6b), the best solution appears for situation 8, with 100 MW of BESS used only for inertial control, while no improvements are seen when the BESS do not contribute to the inertial control (situations 5 and 9). Again the case with 50% of inertial and primary frequency control show a good compromise with sensible improvements with respects to the initial case.

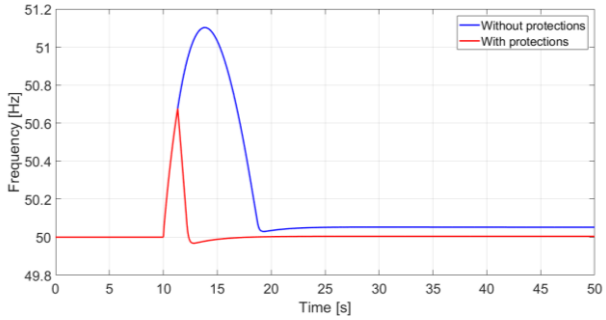

Fig. 7. *Comparisons of the impacts of the worst-case over-frequency contingency for 50% reduced inertia scenario with and without the implementation of actual protection schemes.*

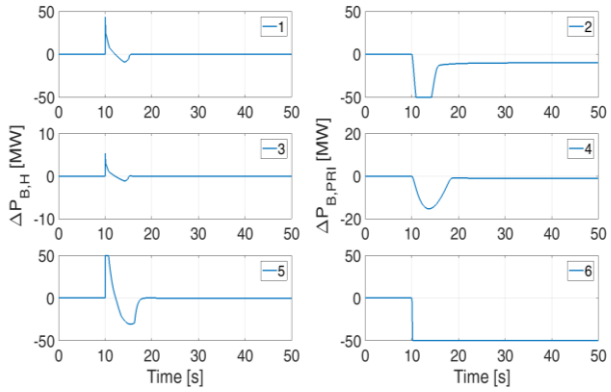

Fig. 8. *Comparisons of the inertial and primary BESS delivered power with the ESL case (1, 2), with lower parameter values (3, 4) and with higher parameter values (5, 6).*

5.2.2 Over-frequency event: The over-frequency event considered is the HVDC SAPEI failure in export.

The comparisons of the failure in the different scenarios show that in the case of 50% of reduced inertia, the situation becomes very critical. Nevertheless, it should be considered that protection schemes are already implemented in actual power systems (Fig. 7). Inspection of Fig. 7 indicates that considering wind shedding, the impacts on the power system stability are less dangerous than expected, but more expensive. In fact the TSO has to pay for the wind power curtailment. In this case, a curtailment of 197.1 MW occurs. The results for the different scenarios are reported in Table 8, only for the most critical 50% reduced inertia scenario, with similar considerations with respect to the ones illustrated for the under-frequency case. The highest improvement in the frequency zenith is 1.61% for the case n = 9, whereas the improvement in the ROCOF is 41.51%, with 10 SyC added.

5.2.3 Comparisons among different logics: The ESL has been compared to other logics to set the parameters H_{BESS} and E_{BESS}. In general, different values can be used for the parameters depending on the control logic. For example, in [13] H_{BESS} varies in the range 0.01 to 500. Here, to easily compare the ESL with other settings, some simulations have been performed starting from the over-frequency event scenario, in the case 6 of Table 3. In particular, the parameters have been changed using ten times lower and higher values. Fig. 8 reports the inertial and primary shares of the BESS delivered power in the ESL case (1, 2), lower (3, 4) and higher (5, 6) values cases. With lower values, the BESS support is not exploited enough, whereas with higher values the saturation of the BESS is reached with possible concerns for the BESS stress and grid stability (especially in the case of ROCOF saturation, when inertia contribution goes to zero). It is evident that the ESL shows the best compromise in terms of BESS saturation and performance.

6. Conclusions

This paper has addressed various theoretical aspects of frequency stability in power system operations:

(i) A power system aggregate model has been constructed to study the impact of SyC and BESSs on the frequency

performance of a real power system, simulating the worst contingency both in over and under frequency.

(ii) Future scenarios in terms of increasing share of renewables have been built and tested, using an optimization approach.

(iii) For the system addressed in the paper, the fast dynamics of the BESS and HVDC enhance the response of the system and are able to counterbalance even a 50% decrease in inertia and regulating energy in the system.

(iv) The results show that both SyC and BESS can improve the frequency response of the power systems. For the BESS, the division of half band for inertial and primary control emerges as the most promising solution. It is shown that in future energy scenarios, only the implementation of virtual inertia is not enough and a fast primary response is needed at the same time.

(v) The average system frequency model is well suited to answer questions concerning the maximum frequency deviation and the time the maximum deviation occurs. It is fast enough to be implemented online for security contingency studies and to carry out extensive parametric studies for system planning purposes. In spite of the model approximations, the comparisons with actual system disturbances are satisfactory. Moreover, the model provides an understanding of the way in which important system parameters affect the frequency response. This understanding is difficult to achieve from high-order models, where many system variables are influent for the system.

The results are satisfactory and depend on the accuracy of dynamic parameters and behaviour of generators and loads, as well as on the system variable estimation, which in turn depends on the quality of the measurements coming from the system. Future works will take into account further considerations for evaluating the proposed methodology from a technical-economic point of view.

7. References

[1] Labisa, P.E., Visandeb, R.G., Pallugnac, R.C., et al.: 'The contribution of renewable distributed generation in mitigating carbone dioxide emissions', Renewable and Sust. Energy Reviews, 2011, 15, (9), pp. 4891-4896.

[2] Ulbig, A., Borsche, T.S., Andersson, G.: 'Impact of Low Rotational Inertia on Power System Stability and Operation', IFAC Proceedings Volumes, 2014, 47, (3), pp. 7290-7297.

[3] Kundur, P.: 'Power System Stability and Control' (McGraw-Hill, New York, 1994).

[4] Arredondo, F., Ledesma, P., Castronuovo, E. D.: 'Optimization of the operation of a flywheel to support stability and reduce generation costs using a Multi-Contingency TSCOPF with nonlinear loads', International Journal of Electrical Power & Energy Systems, 2019, 104, pp. 69-77.

[5] ENTSO-E, 'System Dynamics and Operational Challenges', 2018.

[6] Tielens, P., Van Hertem, D.: 'The relevance of inertia in power systems', Renewable and Sustainable Energy Reviews, 2016, 55, pp. 999-1009.

[7] Liu, Y., Yang, S., Zhang, S., et al.: 'Comparison of Synchronous Condenser and STATCOM for Inertial Response Support'. IEEE Energy Conversion Congress and Exposition, Pittsburgh, PA, USA, Nov. 2014.

[8] Nedd, M., Booth, C., Bell, K.: 'Potential Solutions to the Challenges of Low Inertia Power Systems with a Case Study Concerning Synchronous Condensers'. 52nd International Universities Power Engineering Conference (UPEC), Heraklion, Greece, Aug. 2017.

[9] Mercier, P., Cherkaoui, R., Oudalov, A.: 'Optimizing a Battery Energy Storage System for Frequency Control Application in an Isolated Power System', IEEE Trans. on Power Systems, 2009, 24, (3), pp. 1469-1477.

[10] Nguyen, H.T., Yang, G., Nielsen, A.H., et al.: 'Frequency stability improvement of low inertia systems using synchronous condensers'. IEEE International Conference on Smart Grid Communications, Sydney, Australia, Nov. 2016.

[11] Chen, S., Zhang, T., Gooi, H.B., et al.: 'Penetration rate and effectiveness studies of aggregated BESS for frequency regulation', IEEE Trans. on Smart Grid, 2016, 7, (1), pp. 167-177.

[12] Brivio, C., Mandelli, S., Merlo, M.: 'Battery Energy Storage System for primary control reserve and energy arbitrage', Sust. Energy, Grids and Networks, 2016, 6, pp. 152-165.

[13] Alhejaj, S.M., Gonzalez-Longatt, F.M.: 'Impact of Inertia Emulation Control of Grid-Scale BESS on Power System Frequency Response'. International Conf. for Students on Applied Engineering, Newcastle upon Tyne, UK, Jan. 2016.

[14] Rubino, S., Mazza, A., Chicco, G., et al.: 'Advanced control of inverter-interfaced generation as a virtual synchronous generator'. IEEE Eindhoven PowerTech, Eindhoven, The Netherlands, June 2015.

[15] Brogan, P.V., Best, R.J, Morrow, D.J., et al.: 'Effect of BESS Response on Frequency and RoCoF during Underfrequency Transients', IEEE Trans. on Power Systems, 2019, 34, (1), pp. 575-583.

[16] Toma, L., Sanduleac, M., Baltac, S.A., et al.: 'On the Virtual Inertia Provision by BESS in Low Inertia Power Systems', IEEE International Energy Conference (ENERGYCON), Limassol, Cyprus, Jun. 2018

[17] Ramirez, M., Castellanos, R., Calderon, J.G., et al.: 'Battery Energy Storage for Frequency Support in the BSC Electric Power System'. IEEE PES Transmission and Distribution Conference and Exhibition, Lima, Perù, 2018.

[18] Chan, M.L., Dunlop, R.D., Schweppe, F.: 'Dynamic equivalents for average system frequency behaviour following major disturbances', IEEE Trans. on Power Apparatus and Systems, 1972, PAS-91, (4), pp. 1637-1642.

[19] ENTSO-E, 'Network Code on Load-Frequency Control and Reserves', 2013.

[20] TERNA S.p.A., 'Annex to the grid code A.15 – Participation in the regulation of frequency and frequency/power', 2012.

[21] Andersson, G.: 'Dynamics and Control of Electric Power Systems', ETH Zurich, 2012.

[22] Anderson, P.M., Mirheydar, M.: 'A Low-Order System Frequency Response Model', IEEE Transactions on Power Systems, 1990, 5, (3), pp. 720-729.

[23] Palermo, J.: 'International review of frequency control adaptation'. Australian Energy Market Operator, 2016.

[24] ENTSO-E: 'Network Code on Emergency and Restoration', 2017.

[25] ENTSO-E: 'Network Code for Requirements for Grid Connection Applicable to all generators', 2013.

[26] Zhang, Y. Z.: 'Battery Energy Storage Operation with Adaptive Droop Control', IEEE Conference on Control Technology and Applications, Mauna Lani, HI, USA, Oct. 2017.

[27] EirGrid: 'RoCoF alternative solutions technology assessment: high level assessment of frequency measurements and FFR type technologies and the relation with the present status for the reliable detection of high RoCoF events in a adequate time frame', 2015.

[28] Jomaux, J., Mercier, T., De Jaeger, E.: 'A methodology for sizing primary frequency control in function of grid inertia'. IEEE International Energy Conference, Leuven, Belgium, 2016.

[29] ENTSO-E: ‘Frequency stability evaluation criteria for the synchronous zone of continental Europe’, 2016.
[30] Ghiani, E., Mocci, S., Celli, S., et al.: ‘Increasing the flexible use of hydro pumping storage for maximizing the exploitation of RES in Sardinia’. 3rd Renewable Power Generation Conference, Naples, Italy, Sep. 2014.
[31] Iaria, A., Rapizza, M. R., Marzinotto, M.: ‘Control functions for a radially operated three-terminal VSC-HVDC system: The SA.CO.I. HVDC case’. 2018 IEEE International Conference on Industrial Technology (ICIT), Lyon, France, Feb. 2018.
[32] Drew, D. R., Coker, P. J., Bloomfield, H. C., et al.: ‘Sunny windy sundays’, Renewable Energy, 2019, 138, pp. 870-875.
[33] Ledesma, P., Arredondo, F., Castronuovo, E.: ‘Optimal curtailment of non-synchronous renewable generation on the island of Tenerife considering steady state and transient stability constraints’, Energies, 2017, 10 (11), pp. 1-15.